Journal of The Electrochemical Society



OPEN ACCESS

# The Influence of Some Electrolyte Additives on the Electrochemical Performance of $Fe/Fe^{2+}$ Redox Reactions for Iron/Iron Redox Flow Batteries

To cite this article: Jens Noack *et al* 2021 *J. Electrochem. Soc.* **168** 040529

*Journal of The Electrochemical Society*, 2021 **168** 040529

# The Influence of Some Electrolyte Additives on the Electrochemical Performance of $Fe/Fe^{2+}$ Redox Reactions for Iron/Iron Redox Flow Batteries

**Jens Noack,[1,2,*,z] Max Berkers,[1] Jens Ortner,[3] and Karsten Pinkwart[1,4]**

[1]*Fraunhofer-Institute for Chemical Technology (ICT), 76327 Pfinztal, Germany*
[2]*University of New South Wales, UNSW 2052 NSW Sydney, Australia*
[3]*Wehrwissenschaftliches Institut für Werk- und Betriebsstoffe (WIWeB), 85435 Erding, Germany*
[4]*Hochschule Karlsruhe—Technik und Wirtschaft, 76131 Karlsruhe, Germany*

For the application in Fe/Fe-Redox-Flow-Batteries some important factors concerning the composition of the electrolyte and the influence of temperature on the properties of half-cell reactions were investigated. In contrast to previous investigations, the measurements were performed more realistically on deposited iron and by means of linear sweep voltammetry. Since the distinction between cathodic iron deposition and hydrogen generation is not possible by convention, with quantitative stripping analysis on a rotating disk electrode, partly a method was used to distinguish between these two reactions. The investigations were carried out at temperatures up to 80 °C, with addition of 10 mM of chlorides of Bi, Cu, In, Pb, Sn, Tl, Cd, Sb and Hg and different supporting salts of $NH_4^+$, $Li^+$, $K^+$. $Na^+$, $Cs^+$, $Mg^{2+}$ and $Al^{3+}$.
 [DOI: 10.1149/1945-7111/abf5a3]

Manuscript submitted December 4, 2020; revised manuscript received March 22, 2021. Published April 19, 2021.

Due to technological advancements and economies of scale, the levelized cost of energy (LCOE) from renewable sources has plummeted in the last decade: onshore wind saw an approximately 50% decrease in LCOE between 2010 and 2019, and in the same period the LCOE of photovoltaic generation decreased by as much as 87%.[1,2] As a result, renewable energy generation is already cost-competitive with or even undercutting fossil fuel sources in many parts of the world, and indeed many coal-fired plants—the most expensive type of conventional generation—are being phased out well before the end of their lifetime. However, achieving "deep decarbonization" of the electricity sector to stay within the bounds of the 2015 Paris Climate Agreement requires large-scale energy storage to manage the fluctuations in supply that is inherent in renewable sources dependent on day-and-night cycles and variable weather patterns.[3] Battery Energy Storage (BES) systems have the potential to fulfill the role of grid-scale storage medium, and indeed a significant portion of recently installed storage capacity has been in the form of batteries, particularly of the type lithium-ion (Li-ion), which accounted for 59% of total installed power capacity of all BES systems in mid-2017.[4] The International Renewable Energy Agency (IRENA) projects in its "optimistic" scenarios an increase in total installed storage capacity from 4.7 TWh in 2017 to up to 15.3 TWh in 2030 - an increase of more than 300%.[4] For BES systems specifically, IRENA predicts an order of magnitude increase in capacity growth, from currently estimated 11 GWh to 100–421 GWh in 2030. The USA Department of Energy expects capital costs of 100 USD$/kWh to be market-competitive and has set cost targets for 150 USD$/kWh in 2023.[5] Similarly, the European Union, via its Strategic Energy Technology Plan, has set cost targets for batteries of <150 €/kWh (for a 100 kW system) with a lifetime of thousands of cycles in 2030.[6,7] A class of promising BES technologies is the Redox Flow Battery (RFB). Although RFBs currently made up less than 5% of all installed BES power capacity (in MW) in 2017,[4] RFBs have several advantages that make them attractive for large-scale stationary storage that potentially allows them to become one of the main energy storage techniques in the coming decades.

There are currently dozens of RFB-chemistry candidates under investigation for application in future BES systems.[8–12] One of these promising chemistry candidates is the all-iron hybrid RFB.[13] A configuration for Fe/Fe-RFBs comprises an aqueous solution containing an iron salt such as $FeCl_2$ or $FeSO_4$ as redox-active material, and an electrochemically inert supporting electrolyte salt such as $NH_4Cl$ or NaCl to improve electrolyte conductivity and lower the ohmic losses. During charging of an Fe/Fe-RFB, $Fe^{2+}$ (or "ferrous") ions are oxidized into $Fe^{3+}$ (or "ferric") ions at the positive electrode (see Fig. 1). On the negative or "plating" electrode, ferrous ions are reduced and metallic iron is plated. During battery discharge these processes are reversed: metallic iron is oxidized and dissolves back into the electrolyte on the negative electrode, while ferric ions are reduced to ferrous ions on the positive electrode:

$$\text{Positive electrode: } Fe^{2+} \rightarrow Fe^{3+} + e^- \quad \varphi^{0,+} = +0.77\ \text{V}$$

$$\text{Negative electrode: } Fe^{2+} + 2e^- \rightarrow Fe(s) \quad \varphi^{0,-} = -0.44\ \text{V}$$

$$\text{Cell reaction: } 3Fe^{2+} \rightarrow 2Fe^{3+} + Fe(s) \quad \Delta\varphi^0 = +1.21\text{V}$$

The standard reduction potential of the negative half-cell reaction is 440 mV more negative than that of the hydrogen electrode. Therefore, during charging mode there will also be a reduction of $H^+$ ($H_3O^+$) at the negative electrode where gaseous $H_2$ is formed in the Hydrogen Evolution Reaction (HER):

$$\text{Positive electrode: } Fe^{2+} \rightarrow Fe^{3+} + e^- \quad \varphi^{0,+} = +0.77\ \text{V}$$

$$\text{Negative electrode: } 2H^+ + 2e^- \rightarrow H_2 \quad \varphi^{0,-} = 0.00\text{V}$$

$$\text{Overall HER: } 2H^+ + 2Fe^{2+} \rightarrow 2Fe^{3+} + H_2 \quad \Delta\varphi^0 = 0.77\ \text{V}$$

The HER is considered parasitic, thereby decreasing the round-trip coulombic efficiency and increasing the pH of the negative electrolyte. A possible way to decrease the rate of HER is to increase the pH. However, in Fe/Fe-RFBs the electrolyte pH cannot simply be increased, because at pH ⩾ 2 the ferric ions start to form insoluble hydroxide species that precipitate out of the solution.

Metallic iron is thermodynamically unstable outside of strongly reducing environments, so in acidic media iron tends to slowly dissolve even at open-circuit potential. As a consequence, a charged FeRFB will slowly self-discharge via iron corrosion if the electrolyte is not pumped out of the cell during idle time:

*Electrochemical Society Member.
[z]E-mail: jens.noack@ict.fraunhofer.de

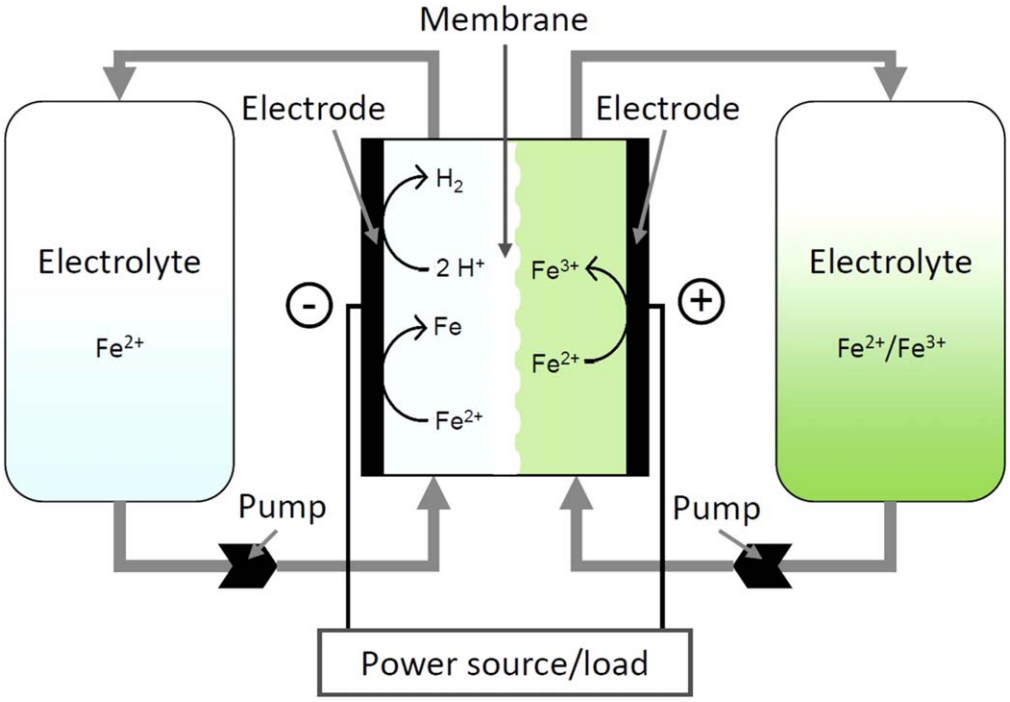


**Figure 1.** Schematics of a Fe/Fe hybrid redox flow battery.

$$2H^+ + 2e^- \rightarrow H_2(g) \quad \varphi^{0,+} = 0.00V$$

$$Fe(s) \rightarrow Fe^{2+} + 2e^- j^{0,-} = -0.44\ V$$

Overall corrosion reaction: $Fe(s) + 2H^+ \rightarrow Fe(s) + H_2(g)$
$\Delta\varphi^0 = 0.44$ V

One strategy to combat the problems caused by increasing pH is to re-combine $H_2$ produced with $Fe^{3+}$ from the positive electrolyte:

Positive electrode: $Fe^{3+} + e^- \rightarrow Fe^{2+} \quad \varphi^{0,-} = 0.00$ V

Negative electrode: $H_2 \rightarrow 2H^+ + 2e^- \quad \varphi^{0,-} = 0.00$ V

Overall re-combination reaction: $2Fe^{3+} + H_2 \rightarrow 2H^+ + 2Fe^{2+}$
$\Delta\varphi = 0.77$ V

Selverston et al. have proposed a cell design where the hydrogen-ferric ion re-combination occurs within the positive electrolyte storage tank by connecting the headspaces of both tanks.[14–17] At low pH the positive $Fe^{2+}/Fe^{3+}$ electrode shows excellent performance, with fast reaction kinetics ($j_0 \approx 10$ mA cm$^{-2}$), high solubility at ambient temperatures (e.g. $[FeCl_2] = 4.9$ M at 20 °C, $[FeCl_3] = 5.6$ M at 25 °C), and no unwanted side-reactions.[13,18,19] Instead, the focus has been on the negative electrode, where the poor $Fe/Fe^{2+}$ kinetics ($j_0 \approx 10^{-8}$ mA cm$^{-2}$) decrease the voltaic efficiency, and the parasitic HER decreases the coulombic efficiency and causes other issues by raising the local and bulk pH. In 2014, Hawthorne et al. studied iron-ligand complexes that could stabilize $Fe^{3+}$ in solutions of pH = 2–3.[20] The authors reported the best results with glycine as ligand. However, complexation with some of these ligands negatively affected the metal solubility and diffusion coefficients. Hawthorne et al. also reported on a study of several factors that affect the negative half-reaction in order to improve the plating efficiency, including pH, supporting salt identity and concentration, and complexation with glycine or glycerol.[21] The authors found that a higher supporting salt concentration inhibits the HER, and that chloride ion suppresses HER more strongly than sulfate ion but at the cost of slower $Fe/Fe^{2+}$ kinetics. Three supporting cations ($K^+$, $Na^+$, and $NH_4^+$) were also compared, with the highest coulombic efficiency of 98% reported for a NaCl-based electrolyte.

Manohar et al. studied two approaches to improve the charging efficiency of the Fe/Fe-RFB.[22] Firstly, limiting the mass-transport of $H^+$ to the electrode surface, and secondly, inhibiting the kinetics of the charge-transfer processes that lead to HER. For the first approach they used with citric acid and ascorbic acid, two complexing agents commonly used in industrial iron-plating and to allow for an operating pH of 2.0 instead of the natural pH of 0.9–1.0 for a solution of 3.0 M $FeCl_2$ and 2.0 M $NH_4Cl$, without precipitation of solid hydroxides. This increased faradaic efficiency from ca. 63% to 83%. The second approach involved the co-deposition of indium or bismuth with iron. A 0.2 M addition of $InCl_3$ to the electrolyte that contained 3 M $FeCl_2$ and 0.3 M ascorbic acid at pH = 2 increased the charging efficiency to 97%. When this electrode was used in flow cell cycling studies, ca. 95% faradaic efficiency was maintained for over 50 cycles. Adding 20 mM $Cd^{2+}$ to a 3 M $FeCl_2$, 2 M $NHCl_4$, 0.3 M ascorbic acid electrolyte increased the coulombic efficiency at higher current densities from 90% to 93%.[23] Investigation of the effect of temperature found that in the range 25 °C–60 °C there was a 0.17% increase in coulombic efficiency per degree Celsius at a charging current of 20 mA cm$^{-2}$.

It is well known in the fields of electrocatalysis and electroplating that the identity of the inert supporting salt can have a significant influence on the kinetics of an electrochemical reaction. Few studies have been done in this area for the hybrid Fe/Fe-RFB. In 1981, Savinell and Hruska briefly examined a few salts by measuring solution conductivity.[13] They noted that $CaCl_2$ is often added in iron-plating baths but in their measurements did not improve solution conductivity, that NaCl and KCl do improve conductivity but yielded deposits of poorer quality, and finally that $NH_4Cl$ both improves conductivity and has good deposit quality. Hawthorne et al.[21] compared $(NH_4)_2SO_4$ and $NH_4Cl$ and found that chloride resulted in lower HER and also demonstrated higher current density and smaller peak separation (i.e., faster kinetics) for the negative electrode reactions. They also compared three cations—namely $K^+$,

$Na^+$, and $NH_4^+$—and found that $NH_4Cl$ had the most negative onset of plating with −0.96 V, −0.84 V, and −0.86 V for $NH_4Cl$, NaCl and KCl electrolytes respectively (all vs Ag/AgCl). $NH_4Cl$ and NaCl produced the most mechanically and chemically stable deposits, with NaCl resulting in pitted surfaces probably due to $H_2$ bubble formation.

The investigation of the redox reactions of $Fe/Fe^{2+}$ is not easy due to the side reaction of hydrogen formation. Furthermore, half-cell studies have been performed in the past on electrode materials other than iron, which is questionable for the interpretation of the results. Finally, deposition in Fe/Fe-RFBs takes place predominantly on deposited iron. For these reasons a range of different electrolytes have been studied under different conditions via voltammetric methods such as cyclic voltammetry and the stripping voltammetric method on a rotating-disk electrode (RDE) described by Hilbert et al.[24] Subjects studied include: operating temperature, the addition of a small amount of a secondary metal to increase HER-overpotential and the influence of the supporting electrolyte salt. The results obtained were compared and discussed with those from the literature.

## Experimental

***Working electrode and working electrode pre-treatment.—***Two kinds of working electrode (WE) have been used in this work, namely glassy carbon (GC, ALS-Japan) and poly-crystalline gold (poly-Au, ALS-Japan). All potentials are referred to the Ag/AgCl reference electrode. Before each experiment, the working electrode was rinsed with ultra-pure Millipore water (18.2 MΩ) and polished with Buehler diamond paste (6, 1, and 0.25 $\mu$m particle size, in that order) with rinsing with Millipore water in between each step. The GC electrode was then placed in an electrolyte containing 2.0 M $NH_4Cl$ and 0.2 M HCl, and was subjected to two potentiodynamic cycles between −1.1 and +1.2 V at 50 mV $s^{-1}$, oxidized potentiostatically by holding the potential at +2.0 V for 30 s, subjected to 20 fast potentiodynamic cycles between −1.2 and +1.2 V at 1000 mV $s^{-1}$, and 2 slow potentiodynamic cycles between −1.2 and +1.2 V at 50 mV $s^{-1}$, and then rinsed with Millipore water. The Au electrode was pre-treated in a 0.1 M $HClO_4$ solution, where it was subjected to 3 potentiodynamic cycles between 0.0 and +1.5 V at 50 mV $s^{-1}$, 50 fast cycles between 0.0 and 1.5 V at 1000 mV $s^{-1}$, and 3 slow cycles between 0.0 and 1.5 V at 50 mV $s^{-1}$, and then rinsed with Millipore water. A Solartron Analytical potentiostat with XM-studio ECS software was used in all experiments for potential control. The experiments were performed with a conventional three-electrode configuration, using a glassy carbon or gold working electrode, platinum wire or disk as counter electrode, and Ag/AgCl reference electrode. For potentiodynamic experiments, a scan rate of 20 mV $s^{-1}$ was found to be a good compromise between level of detail (i.e., resolution) and length of experiments. Voltammograms were recorded as is, without iR-compensation.

***Electrolyte composition and pH control.—***The pH of the electrolyte was adjusted by pipetting a small quantity of $NH_4OH$ solution—or another appropriate hydroxide in the experiments with a supporting cation other than $NH_4^+$—into the electrolyte whilst stirring and actively monitoring the pH with a benchtop pH meter (MettlerToledo, SevenCompact S220). Added volumes of base typically were of the order of <100 $\mu$l in 100 ml solutions, i.e. too small to significantly dilute the concentration of the other solution components. If reference is made to a "standard solution" or "standard electrolyte," this electrolyte had the following composition: 1.5 M $FeCl_2$, 2.0 M $NH_4Cl$, 0.2 M HCl.

***Influence of cationic additives.—***To study the influence of different cation additives on $Fe/Fe^{2+}$ reactions, Linear Sweep Voltammetry (LSV) experiments were carried out at room temperature in electrolytes with the following composition: 2.0 M $NH_4Cl$, 1.0 M $FeCl_2$ and addition of 10 mM $MCl_x$, pH = 2.4, where $MCl_x$ represents an additional metal chloride. Several of the metal chlorides ($BiCl_3$, $PbCl_2$, TlCl, and $SbCl_3$) had such poor solubility or slow dissolution kinetics that even at this low concentration they did not fully dissolve, so the actual concentration was lower than 10 mM. The stationary WE had been covered directly prior to the LSV step by plating for 30 s at a constant potential of −1.2 V, and the potential was then swept with 20 mV $s^{-1}$ from the open circuit potential into either the cathodic direction up to −1.2 V, or in the anodic direction up to +0.7 or +0.8 V. Au was used as working electrode for most metals. However, for the Hg experiment a GC working electrode was used since Hg as a strong tendency to form amalgams with Au.

### Quantitative Anodic Stripping analysis using a Rotating Disc Electrode (RDE)

Measuring the properties of the redox reactions of $Fe/Fe^{2+}$ has several difficulties:

(i) the measured currents (or potentials) are very irregular due to formation of non-conductive $H_2$-bubbles that block parts of the surface and thereby prevent plating or dissolution;
(ii) the deposition rate changes as the electrode surface gets covered with iron, i.e. the deposition rate is not constant but depends on plating duration because of the change of the material of the substrate
(iii) for GC electrodes specifically, the iron deposit is of poor quality and tended to physically dislodge from the surface.

Therefore a variation of an anodic stripping voltammetry method, devised by Hilbert and coworkers,[24] was used, which will be referred to as Quantitative Anodic Stripping (QAS). A rotating disk-electrode (RDE) is used to ensure that the near-electrode concentration of $H^+$ and $Fe^{2+}$ remains stable and near the bulk concentration, and $H_2$-bubbles are physically dislodged and flung away from the surface. After plating at a constant potential for a brief period $t_1$, a steady-state plating current should be reached. If $t_1$ is known, in a repeat experiment the potential can be increased at $t_1$ to one more positive than the corrosion potential to strip the plated metal. The "non-steady-state" charge $Q_1$ corresponding to this stripping current is recorded. In subsequent experiments, the metal is plated for a period $t_2$ (which is longer than $t_1$) and then stripped, yielding $Q_2$, proportional to the amount of metal plated. The steady-state partial current for the plating reaction can then be calculated according to:

$$i_{Fe} = \frac{Q_2 - Q_1}{t_2 - t_1}$$

And the partial current density for the HER can be then obtained simply by subtracting the plating current from the total cathodic current:

$$i_{HER} = i_{tot} - i_{Fe}$$

The working rotating-disk electrode was a 5.0 mm diameter polycrystalline Au disk (Pine Research) and mounted in a rotator (Princeton Applied Research, model no. 636 A). Before each run, the Au-RDE was stripped of any residual iron by applying a "stripping" potential of +0.35 up to +0.75 V for a duration of 30 up to 60 s, followed by the QAS procedure run in triplicate or quadruplicate. The QAS procedure comprised a 60 s potentiostatic plating step at a given potential, followed by an "equilibration" step where the potential was held at open-circuit potential for 1 s, a potentiodynamic linear sweep in anodic direction from the open circuit potential to +0.35 V at a scan rate of 20 mV $s^{-1}$, and finally by a stripping step identical to the one used before the start of the experiment to clear any residual iron.

***Scanning electron microscopy.***—A gold wire of ca. 500 $\mu$m diameter was used as working electrode and plated with iron and indium from a solution of pH = 2.4, 1.0 M $FeCl_2$, 2.0 M $NH_4Cl$ and 1 mM $InCl_3$ by holding the potential at −1.2 V for 120 s, followed by 60 s at open circuit potential, followed by another 120 s at −1.2 V. The wire was then cut transversally, exposing a cross-section of the wire and plated mantle. Micrographs were obtained on a Scanning Electron Microscope using an acceleration voltage of 15 kV, and an electron beam current of 0.4 nA. Energy dispersive X-ray Spectrometry (EDX) was used for elemental identification.

## Results and Discussion

***Temperature effects.***—Figure 2 depicts cyclic voltammograms curves recorded on GC in the standard electrolyte under $N_2$ atmosphere at different elevated temperatures. The mixed iron deposition and HER currents are very irregular due to high rate of HER forming bubbles on the surface. There are three obvious effects caused by higher temperatures. First, the onset of the mixed HER and iron deposition current shifts to more positive values, indicating lower nucleation overpotential. Second, the peak area of iron oxidation increases with higher temperature, as more iron is deposited during the deposition step. As a consequence of these first two observations the coulombic efficiency increases with increasing temperature, yielding efficiencies of 43.6%, 46.5% and 52.2% respectively for 60 °C, 70 °C and 80 °C. Third, the $Fe^{2+}/Fe^{3+}$ reaction also has somewhat higher current densities, although there is no change in onset potential. All three observations suggest that increasing the operating temperature would be favorable for the Fe/Fe-RFB.

Cyclic voltammetry and linear sweep voltammetry experiments were carried out on a static poly-Au WE that had been covered with Fe directly prior to the sweep by plating for 30 s at a constant potential of −1.2 V (Fig. 3). This pre-plating step was expected to yield more meaningful data, because Fe was plated from solution on Fe instead on Au, which will more closely resemble real-world conditions, as in a practical battery the electrode will quickly get covered with Fe and the deposition process is most of the time Fe on Fe.

In the cathodic sweep (Fig. 3a), the higher electrolyte temperature leads to an earlier onset of the cathodic current, with a decrease in overpotential of about 160 mV at 80 °C compared to 25 °C. Note that this is not the nucleation overpotential but the actual plating overpotential, thanks to the pre-plating step. With this experimental set-up, the individual contributions of the concurrent HER and Fe-deposition reaction were impossible to determine accurately, because the formation of non-conductive $H_2$-bubbles on the electrode surface resulted in very irregular currents.

In the anodic sweep (Fig. 3b), higher temperatures caused the dissolution peaks to increase in size because a larger quantity of iron had been deposited during the plating step, from 4.9 C $cm^{-2}$ at 25 °C to 25.2 C $cm^{-2}$ at 80 °C, a roughly fivefold increase (Table I). This demonstrates that the increase in cathodic current due to elevated temperature was caused at least partly by a significant increase in Fe-deposition rate. There was no apparent increase in coulombic efficiency with increased temperature (Table I), however this method did not yield the most reproducible numbers due to the vigorous HER during plating. Unlike the reduction reactions, there was no decrease in overpotential for the metal dissolution upon increasing the temperature.

The Quantitative Anodic Stripping (QAS) method was applied to 1.5 M $FeCl_2$, 2.0 M $NH_4Cl$, pH = 2.0 electrolytes of different temperatures using a poly-Au RDE rotating at 2000 rpm, the results of which are depicted in Fig. 4. At 25 °C, the Fe deposition current had its onset at −0.85 V, corresponding to ca. 0.24 V overpotential. Increasing the temperature to 50 °C shifted the onset of the Fe deposition current in positive direction by ca. 60–75 mV. This should result in a significant improvement in performance in a practical battery, which typically runs in constant current mode, because at a given charging current (e.g. −100 mA $cm^{-2}$), the applied potential will be significantly less negative (Fig. 4a), yielding a higher voltaic efficiency. Like the Fe deposition current, the HER current was also higher at more negative potentials, but the initial rise in Fe deposition current around −850 mV was much steeper. As a consequence, at 25 °C the coulombic efficiency for iron plating increased from 0% at −700 mV, to 48% at −900 mV, to 89% at −1100 mV (Fig. 4b).

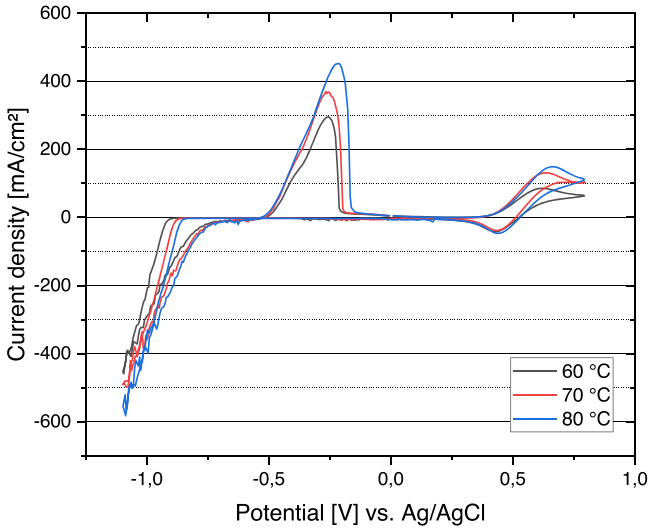


**Figure 2.** Cyclic voltammograms recorded on a static glassy carbon working electrode. Electrolyte composition was 2.0 M $NH_4Cl$, 1.5 M $FeCl_2$, 0.1 M HCl, under $N_2$ atmosphere. Curves were recorded at 20 mV $s^{-1}$, starting at 0.0 V in positive direction, with vertex potentials of +0.8 V and −1.1 V. Only the second cycle of each CV is depicted. (Color figure available in online version at Journal of The Electrochemical Society).

Shifting the plating potential even further negative, marginally increased the coulombic efficiency, however in this experimental configuration the coulombic efficiency seems to plateau at ca. 90%. Both the HER and Fe deposition currents at a given potential are increased by raising the temperature, but this effect was stronger for the Fe deposition current, so the coulombic efficiency at a given potential was higher at elevated temperatures (Fig. 4b).

***Effects of different metal additives.***—Figure 5 shows LSVs of Fe electrolytes with different metal additives. In the cathodic sweep (Fig. 5a) all curves showed similar behavior. Some of the investigated metal ions had a plating onset that was much earlier than that of Fe, e.g. Cu around −0.26 V, which should result in electrode coverage by several monolayers of secondary metal before the onset of Fe deposition and HER. Other metals had a plating onset much closer to that of Fe, e.g. Cd around −0.75 V which can be seen in Fig. 5a in the form of a small peak. Most notable among the cathodic curves are Sn and In which had a much earlier onset, and Pb and Cd which had a much later onset. To what extend this was caused by inhibition or enhancement of either the HER or Fe deposition could not be determined with simple LSV experiments and requires the use of QAS-analysis. In the anodic sweep the different effects of the secondary metals were more apparent (Fig. 5b).

On Au, most metals (except for Bi) had a positive effect on the amount of metal plated compared to the additive-free electrolyte, resulting in larger dissolution peaks. The highest metal dissolution peaks were obtained with Tl, Cd and Sb, which increased the amount of metal plated (in Coulombs) by ca. 80% (Fig. 7). The metals Cu, Bi, Cd, Pb and Tl also seemed to have a positive effect on the $Fe^{2+}$ oxidation reaction, whereas In increased the overpotential and Sn and Sb completely inhibited it. These findings might explain why the Narayanan group switched from using In and Bi as additives in their 2016 paper,[22] to using the much more toxic Cd in their 2018 paper.[23] Hg was the only metal tested on GC working electrode (see Fig. 6)

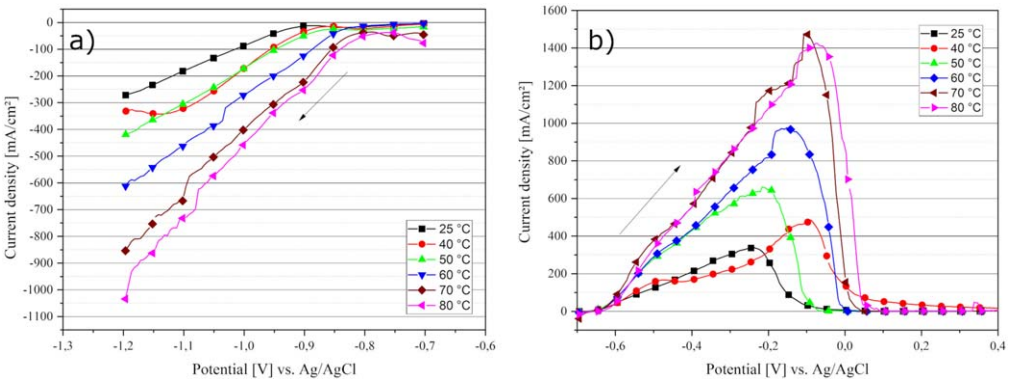


**Figure 3.** Linear sweep voltammograms on poly-Au WE pre-plated with Fe from pH = 2.4 solution of 1.5 M $FeCl_2$ and 2.0 M $NH_4Cl$. After plating for 30 s at −1.2 V, the potential was swept from −0.7 V in the cathodic (a) or anodic (b) direction at a sweep rate of 20 mV $s^{-1}$.

**Table I. The amount of iron oxidized in the anodic sweep of Fig. 3, in terms of charge; coulombic efficiency of the plating step calculated by dividing the metal oxidation current in Fig. 3b by the total charge passed in the plating step prior to the linear sweep of Fig. 3b.**

| Temperature [°C] | Charge [C $cm^{-2}$] | Coulombic Efficiency [%] | $i_{P,A}$ [mA $cm^2$] | $i_{P,C}$ [mA $cm^{-2}$] |
|---|---|---|---|---|
| 25 | 4.9 | 92.2 | 341 | 271 |
| 40 | 8.2 | 81.5 | 480 | 343 |
| 50 | 10.5 | 91.5 | 655 | 418 |
| 60 | 16.2 | 94.7 | 968 | 609 |
| 70 | 23.6 | 91.3 | 1476 | 854 |
| 80 | 25.2 | 93.7 | 1421 | 1033 |

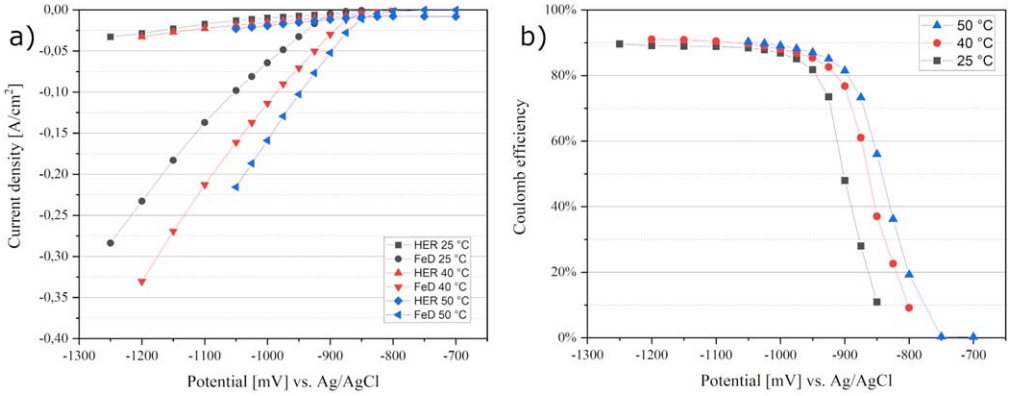


**Figure 4.** Quantitative anodic stripping voltammetry recorded on poly-Au RDE rotating at 2000 rpm in electrolyte with composition 2.0 M $NH_4Cl$, 1.5 M $FeCl_2$, pH = 2.0. (a) Partial current density vs applied potential at different temperatures for HER and Fe deposition; (b) Coulombic efficiency vs potential. Each data point is the average of four measurements.

because of the strong tendency to form amalgams with Au, and showed a decrease of −25% in terms of the total amount in coulombs of plated metal (which includes both Fe and Hg).

In summary, these results suggest that Cu, Pb, Tl and Cd could be promising additives to improve the coulombic efficiency of the Fe deposition reaction without negatively affecting the $Fe^{2+}/Fe^{3+}$ reaction. However, a more precise quantification using QAS analysis is necessary to gain more insight in the mechanism by which these metals improve the amount of iron plated. Figure 7 shows the amount of charge for the dissolution process of iron. Tl, Cd and Sb additives resulted in the highest charge densities followed by Cu, In, Pb an Sn. Bi resulted surprisingly in the lowest charge density and Hg also resulted in a lower charge density than without the additive.

Two recent papers on the hybrid Fe/Fe-RFB by the Narayanan group involved the co-deposition of a secondary metal with Fe to improve coulombic efficiency.[22,23] The authors postulate that these metals (In, Bi and Cd) will remain at the electrode surface and will not diffuse into the bulk of the plated iron because of their theoretical immiscibility with iron. Therefore, only a small amount of secondary metal is necessary to nearly completely inhibit the HER, since there always remain a few monolayers of secondary metal at the surface.

However, the authors presented no evidence to support this mechanism of action. Therefore, an attempt was made to confirm this hypothesis by plating a thin gold wire with iron ($[Fe^{2+}]$ = 1.0 M) and indium ($[In^{3+}]$ = 0.01 M), and use electron microscopy combined with EDX to determine whether indium accumulates at the surface or is distributed homogeneously throughout the deposit. Iron was deposited on Au in a step of 120 s of plating at −1.2 V, followed by 60 s of keeping the potential at open circuit, followed by another plating step of 120 s. Unfortunately, the concentration of In turned out to be so low that it mostly fell below the detection limits of the EDX, so it could not be determined if In was incorporated in the metal as an alloy or aggregated on the metal surface. At the Au-

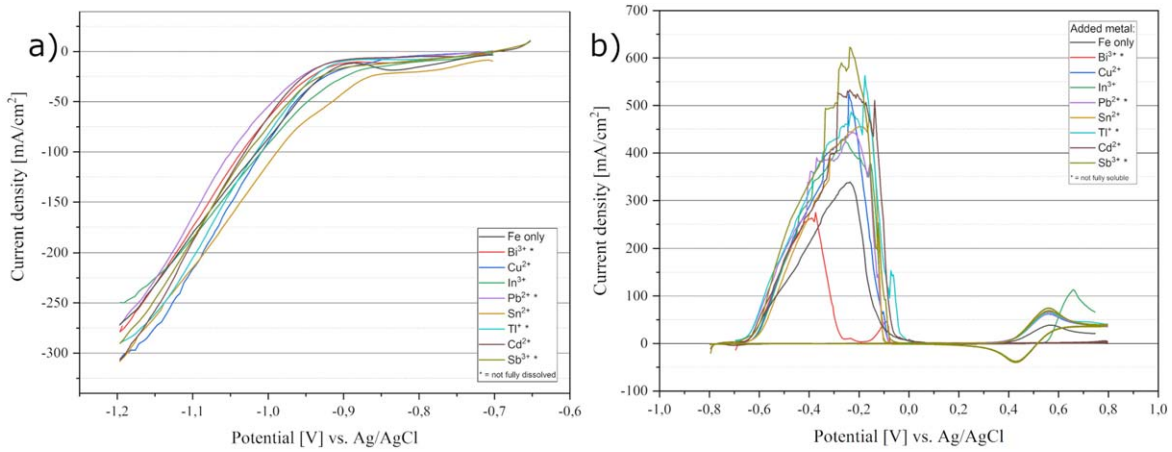


**Figure 5.** Linear sweep voltammogram recorded on a stationary Au electrode that had been plated with metal by applying −1.2 V potential for 30 s directly prior to sweep voltammetry. Electrolyte composition: 2.0 M $NH_4Cl$, 1.0 M $FeCl_2$, addition of 10 mM $MCl_x$, pH = 2.4, where $MCl_x$ represents an additional metal chloride. (a) Potential was swept from −0.7 V in negative direction at a scan rate of 20 mV $s^{-1}$. (b) Linear sweep voltammogram in anodic direction at 20 mV $s^{-1}$. Asterisks indicate that the additional metal did not fully dissolve. (Color figure available in online version at Journal of The Electrochemical Society).

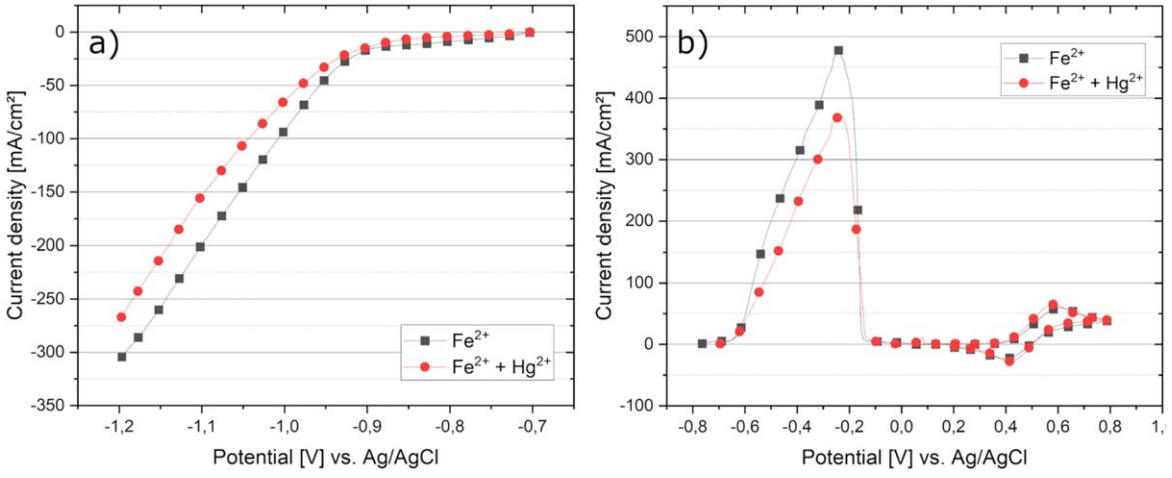


**Figure 6.** Linear sweep voltammogram recorded on stationary GC electrode that had been plated with metal by applying −1.2 V potential for 30 s directly prior to sweep voltammetry. Electrolyte composition: 2.0 M $NH_4Cl$, 1.0 M $FeCl_2$, 10 mM $HgCl_2$, pH = 2.4. (a) Potential was swept from −0.7 V in negative direction at a scan rate of 20 mV $s^{-1}$. (b) Linear sweep voltammogram in anodic direction at 20 mV $s^{-1}$.

Fe interface, there was no detectable amount of indium, but at the Fe–Fe interface a clear localization of In could be observed (Fig. 8). This could be caused by In aggregating on the surface during the first plating step as Narayanan and coworkers claim, by the fact that In deposition occurs at slightly less negative potentials than Fe deposition and will therefore plate before Fe, or both.

***Effects of different supporting electrolyte cations.—***To study the influence of the cation on the $Fe/Fe^{2+}$ and HER reactions, linear sweep voltammograms were recorded on an Au working electrode that was pre-coated with Fe by plating for 30 s at −1.2 V. In the cathodic sweeps, depicted in Fig. 9a, there was a large difference in the onset potentials of the cathodic current, with the earliest (i.e., most positive) onset potential observed in $K^+$-based electrolyte, and the latest (i.e., most negative) onset potential in $Cs^+$ and $NH_4^+$-based electrolyte. The $Mg^{2+}$ electrolyte in particular resulted in much lower currents than the other cations. From these voltammograms, it cannot be determined what proportion of the current is due to either Fe deposition or HER. However, if the earlier onset seen with $K^+$ is due to a lower overpotential of Fe deposition, that would be very favorable as it would result in better voltaic efficiency for the charging step, and if the HER overpotential is not increased (as much) it will result also in better coulombic efficiency.

In the anodic sweeps, depicted in Fig. 9b, the ammonium and caesium based electrolytes had the earliest (i.e., most negative) onset potential, which is exactly the reverse of what was observed in the cathodic sweep, suggesting that $NH_4^+$ and $Cs^+$ shift the equilibrium potential more negative than the other cations. All other factors being equal, a more negatively shifted equilibrium potential would yield a higher overall cell potential, and therefore a higher energy density. The highest amount of Fe dissolved in the anodic sweep are achieved with $Li^+$ and $Na^+$ electrolyte, while the electrolytes with $Mg^{2+}$, $Al^{3+}$ and $Cs^+$ perform poorer than the commonly used $NH_4^+$ (Fig. 10a).

Since the cations can influence both, the overpotentials of the different reactions, as well as the equilibrium potential, it becomes less straightforward to predict how each cation will perform in a battery. If a cation shifts the equilibrium potential by increasing the overpotential of the forward reaction but decreasing the overpotential for the reverse reaction by the same amount, the overall voltaic efficiency might be unaffected (although the overall cell potential is increased or decreased). Figure 10b lists the different cations with an approximation of their onset potential in the form of the potential where the current density is ±15 mA $cm^{-2}$ in the LSVs depicted in Figs. 9 and 10a, as well as the difference between the two for an estimation of the overpotential difference for $Fe/Fe^{2+}$ redox

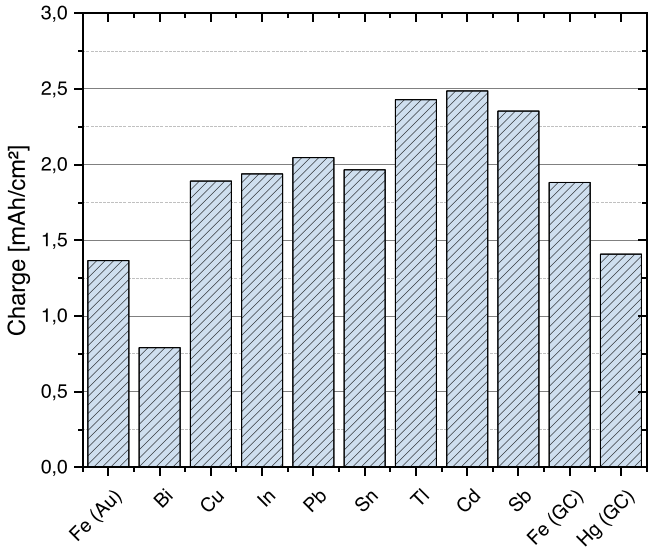


**Figure 7.** Total charge under the anodic metal dissolution curves of Figs. 5b and 6b. Type of working electrode in brackets. If not stated, working electrode was Au.

To study the effect of the supporting salt on the HER and plating reaction separately, a QAS experiment was set up on an Au RDE working electrode. The electrolyte consisted of 2.0 M XCl, 1.5 M $FeCl_2$, at pH = 2.0, where X = $Li^+$, $K^+$, $Na^+$ or $NH_4^+$. The results are shown in Fig. 11. In terms of HER, all four cations exhibited a similar response. On the other hand, for the plating reaction it is clear that $Li^+$ and $Na^+$ had an earlier onset for iron plating (Fig. 11a), and consequently they had higher coulombic efficiency at low overpotentials (Fig. 11b). These results should translate into higher voltage efficiency in battery cycling tests, which are run in constant-current mode. There is some disagreement between these findings and those of Hawthorne,[56] who found that $K^+$ and $Na^+$ both resulted in ca. 100 mV more positive plating onset potentials than $NH_4^+$. But those results were obtained via cyclic voltammetry on a Cu working electrode, whereas the results shown in Fig. 11 were obtained on an iron-covered Au RDE.

## Conclusions

The effect of elevated temperature was studied, in which it was found that increasing the electrolyte temperature decreased the iron deposition overpotential and increased both the iron deposition and hydrogen evolution rate. Increasing the operating temperature from 25 °C to 50 °C decreased the plating potential by approximately 50 mV, and increasing the temperature further to 80 °C resulted in a

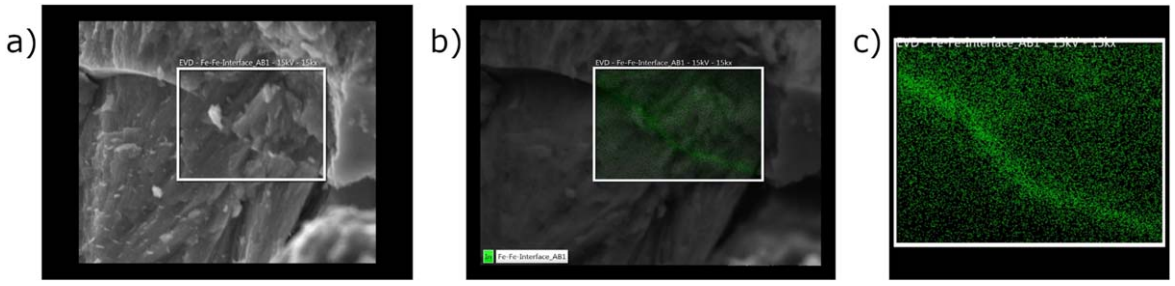


**Figure 8.** Elemental mapping via EDX of the Fe–Fe interface plated from electrolyte with 2.0 M $NH_4Cl$, 1.0 M $FeCl_2$, 10 mM $InCl_3$.

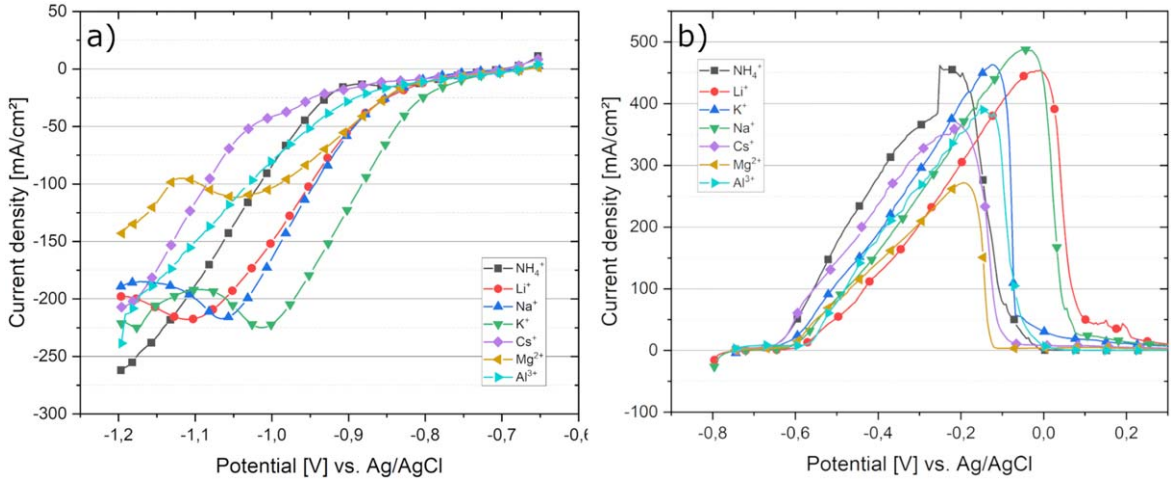


**Figure 9.** Linear sweep voltammograms recorded on an Au working electrode after plating for 30 s at −1.2 V in electrolyte containing 2.0 M chloride salt, 1.0 M $FeCl_2$ at pH = 2.0. (a) The potential was swept with 20 mV $s^{-1}$ from −0.65 in the negative (cathodic) direction; (b) the potential was swept with 20 mV $s^{-1}$ from −0.80 V or −0.75 V in the positive (anodic) direction.

reactions. The lowest values for the overpotential difference were obtained in $K^+$ and $NH_4^+$ electrolytes, with a difference of 159 and 194 mV, respectively. These cations would be expected to result in the highest voltaic efficiency. The electrolytes with $Na^+$ and $Li^+$ had comparatively high overpotential differences and thus probably lower voltage efficiencies in a battery, although they achieved higher charge quantities.

150 mV lower overpotential. Quantitative anodic stripping voltammetry experiments at different temperatures revealed that both the hydrogen evolution reaction and iron plating reaction are enhanced by the elevated temperature, but this increase was stronger for the latter reaction, leading to higher coulombic efficiencies at lower overpotential.

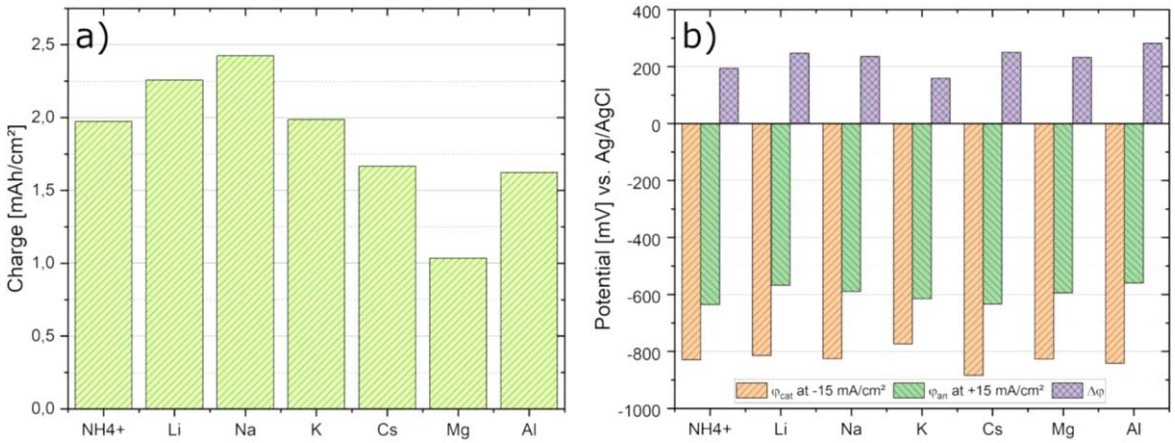


**Figure 10.** (a) Total amount of metal plated (in units of charge) obtained by integrating anodic sweep depicted in Fig. 9 between −0.70 and +0.35 V, before the onset of $Fe^{2+}$ oxidation. (b) Influence of supporting cation on onset potentials and overpotential difference in the linear sweep voltammogram.

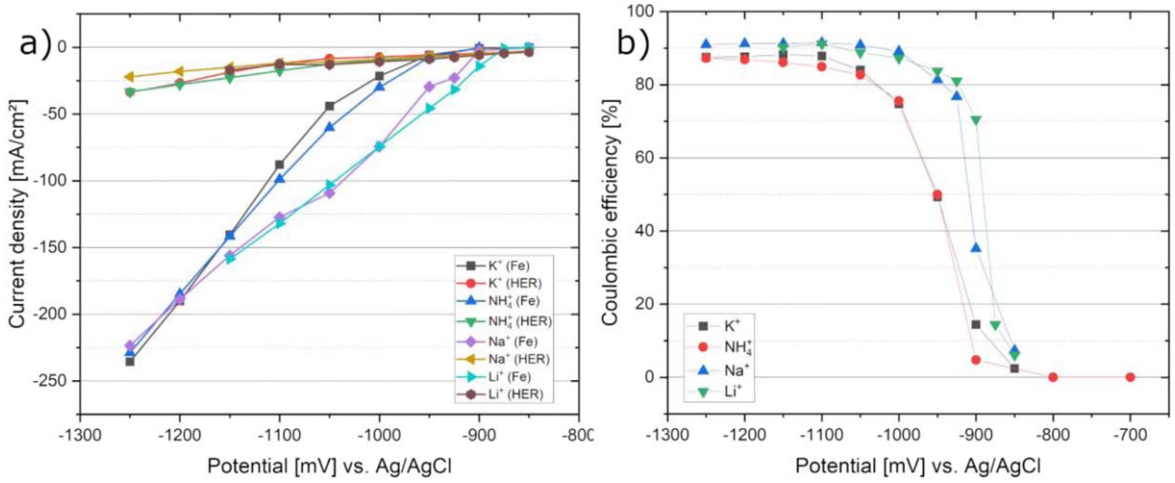


**Figure 11.** Partial current density of HER and Fe deposition (a), and the corresponding coulombic efficiency (b). Data obtained by quantitative anodic stripping voltammetry method on a Au RDE rotating at 2000 rpm, with plating time of 30 s, in electrolyte of 2.0 M XCl, 1.5 M FeCl2, pH = 2.0. Each data point is the average of four scans.

To choose the best supporting electrolyte, several salts were studied: either chloride salts with various cations, or ammonium salts with various anions. It was found that of the cations $Li^+$, $NH_4^+$, $Na^+$, $K^+$, $Cs^+$, $Mg^{2+}$ and $Al^{3+}$, the best results regarding Fe dissolution capacity were obtained with $Na^+$ and $Li^+$ as supporting cation. Electrolytes containing these cations decrease the iron plating overpotential by up to 80 mV without significantly increasing the hydrogen evolution rate, resulting in higher coulombic efficiencies. Electrolytes with $K^+$ resulted in a lower Fe dissolution capacity than $Li^+$ and $Na^+$ but also in a much lower onset potential difference for the $Fe/Fe^{2+}$ redox reaction. Therefore, $K^+$ is also an interesting option for higher voltage efficiencies.

The addition of low concentration (10 mM) of secondary metal chlorides was studied as a potential method to selectively inhibit the hydrogen evolution reaction. Eleven metals were selected that both had the ability to co-plate or alloy with iron, and have a lower exchange current density for hydrogen evolution than iron. Among the metals that were investigated, the most promising candidates were Cu, Tl, Pb and Cd. The best results were obtained with the Cd electrolyte, yielding up to 80% more metal plated (in $C/cm^2$) than the iron-only electrolyte under identical conditions. Notably, some metals like Sn and Sb inhibited the $Fe^{2+}/Fe^{3+}$ reaction, highlighting the need to always investigate this reaction as well when studying methods to improve the $Fe/Fe^{2+}$ reactions.

The investigations have shown that there is a high development and innovation potential for the electrolyte. Within the scope of this work, only a few additives with one concentration could be investigated. However, concentration series would be much more meaningful and offer an interesting field for optimization in addition to other additives and the behavior of the composition of multi-component mixtures. In particular, hydrogen formation and the associated dynamics due to changing pH-value at the electrode, combined with the potential precipitation of hydroxides, remains another important subject of investigation for enabling durable Fe/Fe-RFBs.

## Acknowledgments

The authors would like to thank the German Federal Ministry of Defence (BMVg) for financing this project.

## ORCID

Jens Noack https://orcid.org/0000-0002-0885-5762

## References

1. International Renewable Energy Agency (IRENA), (2020), 10 Years: Progress to Action.
2. International Renewable Energy Agency (IRENA), (2018), Renewable Power Generation Costs in 2018.
3. D. Gielen et al., *Energy Strategy Reviews*, **24**, 38 (2019).

4. International Renewable Energy Agency (IRENA), (2017), Electricity storage and renewables: Costs and markets to 2030.
5. Grid Energy Storage, (2013), December 2013 [cited 2020 01-June]; Available from: (https://energy.gov/oe/downloads/grid-energy-storage-december-2013).
6. European Commission, (2011) p. 46Materials Roadmap - Enabling Low Carbon Energy Technologies https://setis.ec.europa.eu/system/files/Materials_Roadmap_EN.pdf.
7. European Association for Storage of Energy (EASE), (2017), European Energy Storage Technology Development Roadmap - Update.
8. E. Sánchez-Díez et al., *J. Power Sources*, **481**, 228804 (2021).
9. C. Zhang et al., *Energy Storage Mater.*, **15**, 324 (2018).
10. M. V. Holland-Cunz, F. Cording, J. Friedl, and U. Stimming, *Front. Energy*, **12**, 198 (2018).
11. Y. Ding, C. Zhang, L. Zhang, Y. Zhou, and G. Yu, *Chem. Soc. Rev.*, **47**, 69 (2018).
12. Q. Zhao, Z. Zhu, and J. Chen, *Adv. Mater.*, **29**, 1607007 (2017).
13. L. W. Hruska and R. F. Savinell, *J. Electrochem. Soc.*, **128**, 18 (1981).
14. S. Selverston, E. Nagelli, J. S. Wainright, and R. F. Savinell, *J. Electrochem. Soc.*, **166**, A1725 (2019).
15. S. Selverston, R. F. Savinell, and J. S. Wainright, *J. Power Sources*, **324**, 674 (2016).
16. S. Selverston, *Iron-based flow batteries: Improving lifetime and performance, in Department of Chemical and Biomolecular Engineering* (Case Western University, Cleveland, Ohio) (2017).
17. S. Selverston, J. S. Wainright, and R. Savinell, *Sealed aqueous flow battery systems with in-tank electrolyte rebalancing*, US20180294502A1 (2018).
18. K. L. Hawthorne, J. S. Wainright, and R. F. Savinell, *ECS Trans.*, **50**, 49 (2013).
19. K. L. Hawthorne and R. F. Savinell, *ECS Trans.*, **41**, 35 (2012).
20. K. L. Hawthorne, J. S. Wainright, and R. F. Savinell, *J. Electrochem. Soc.*, **161**, A1662 (2014).
21. K. L. Hawthorne, T. J. Petek, M. A. Miller, J. S. Wainright, and R. F. Savinell, *J. Electrochem. Soc.*, **162**, A108 (2015).
22. A. K. Manohar et al., *J. Electrochem. Soc.*, **163**, A5118 (2016).
23. B. S. Jayathilake, E. J. Plichta, M. A. Hendrickson, and S. R. Narayanan, *J. Electrochem. Soc.*, **165**, A1630 (2018).
24. F. Hilbert, Y. Miyoshi, G. Eichkorn, and W. J. Lorenz, *J. Electrochem. Soc.*, **118**, 1927 (1971).